CHAPTER 2

Synthesis of Magnetite, Magnetite- Silver Core-Shell Nanostructure and their Structure

2.1 Introduction

While numerous methods of nanoparticle synthesis have been developed, their successful application is highly dependent on the stability of these particles under various conditions [83,112-114].

The bare metallic nanoparticles (NPs) are chemically highly unstable and tend to form agglomerates that lead to loss in magnetic and optical properties thus, it becomes crucial to overcome these drawbacks and develop protection strategies by functionalizing or coating these bare nanoparticles using some chemically stable metal-organic frameworks, dyes or polymers [115-117]. Moreover, these functionalized nanoparticles, apart from being chemically stable and dispersible, tend to offer excellent physical and chemical properties which can be exploited in order to widen and excel their applicability [118-120].

Magnetite is one of the most studied iron oxide having chemical formula Fe_3O_4. It is chemically known as ferrous-ferric oxide as it contains both divalent and trivalent Fe cations. Due to its excellent physical and magnetic properties, it has been used successfully for varying applications like magnetic data recording, sensors, transformer cores, water remediation and multiple areas of biology and medicine in its both bulk and nanostructured form. Here, details of some important iron oxides and magnetite are presented.

2.2 Iron Oxide Nanoparticles and their Properties

Iron oxide nanoparticles are the nanoparticles that consist of iron and oxygen ions. There are overall 16 known types of iron oxides as well as oxyhydroxides [121]. Out of these, three are considered as important ones: hematite, maghemite and magnetite. Hematite crystallizes into the rhombohedral crystal system with space group $R\bar{3}c$ and Fe (III) ions [122]. It shows antiferromagnetic behavior below Morin transition (at 250 K), canted antiferromagnetism or weak ferromagnetism up to the Néel temperature (at 948 K) and above, Néel temperature, it is paramagnetic [123]. The structure of maghemite and magnetite are very much similar and show ferrimagnetic spin ordering. The ferric ions along with vacancies occupy the octahedral sites in case of maghemite. It shows a ferrimagnetic behavior with Néel temperature ~ 950 K [94,124].

2.3 Structure and Magnetic Properties of Magnetite

The magnetite crystallizes in cubic inverse spinel pattern with chemical composition $Fe^{2+}Fe_2^{3+}O_4^{2-}$. The oxygen ions form cubic closed packing (ccp) structure with iron ions occupying the voids, octahedral and tetrahedral, formed in between the oxygen ions. The tetrahedral voids are filled with half of the ferric ions whereas the octahedral sites are occupied by other half ferric ions as well as equal number of ferrous ions. There are 32 O^{2-} ions in one unit cell with lattice constant ~0.839 nm, with 8 formula units present in each unit cell of magnetite. The unit cells of magnetite adhere to face-centered cubic pattern [125]. The metal ions are located at Wyckoff positions 8a, 16d whereas the anion is located at Wyckoff site 32e of Fd3m space group. The atomic positional coordinates of these ions can be given as (0.1250, 0.1250, 0.1250), (0.5000, 0.5000, 0.5000) for metal ions and (u-0.125, u-0.125, u-0.125) for oxygen, where u is known as oxygen parameter. The structure of magnetite is shown in figure 2.1.

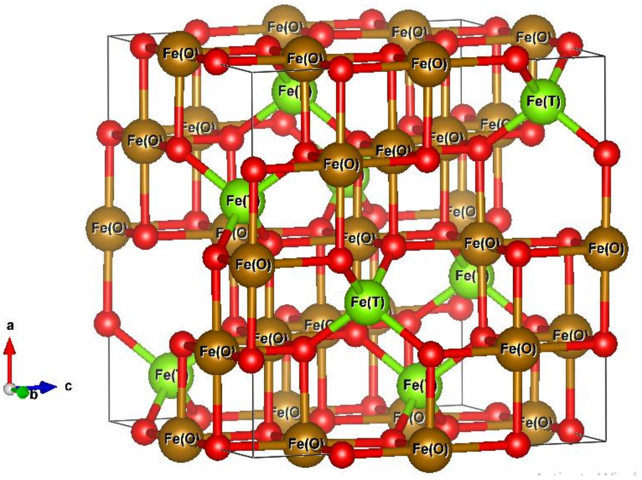

Figure 2.1 Structure of magnetite unit cell

In 1939, a fundamental discovery was made by Verwey which reported that magnetite experiences a sharp and first order transition when cooled below ~120 K, at which the conductance of sample shows a discontinuous drop. This transition has been termed as Verwey transition and was shown to be stoichiometric dependent [126]. In context to the magnetic properties, magnetite exhibit Curie temperature at 850 K above which it shows paramagnetic behavior. Below 850 K it shows ferrimagnetic ordering. The magnetite nanoparticles shown to be in the single domain below a size of 50 nm and superparamagnetic below 20 nm for relaxation time τ_s=100 s at room temperature [127-130]. These limits crucially depend on the synthesis technique used for obtaining the magnetite nanoparticles. We will describe some of the widely used synthesis methods for obtaining magnetite nanoparticles in the following section.

2.4 Synthesis of Magnetite Nanoparticles using Various Techniques

The researchers have tried to synthesize the magnetite nanoparticles using several methods such as co-precipitation, thermal decomposition, chemical vapor deposition, combustion, laser pyrolysis, microemulsion and microwave-assisted techniques.

The co-precipitation of products in the solutions is one of the earlier techniques to prepare nanoparticles. In this method, the magnetic nanoparticles are obtained from aqueous solutions of salts by adding a base at room temperature or high temperature under an inert atmosphere. The size and shape of obtained nanoparticles can be controlled by the use of different types of salts, pH value, ratio of ferrous and ferric salts, concentration as well as the reaction temperature. The Fe_3O_4 nanoparticles in size range 10-40 nm has been reported by several groups using co-precipitation method [131-132]. The most promising methods for formation of uniform sized nanoparticles commonly used in biological applications, is reported to be the polyol method. In this technique, the metallic salts are reduced into fine metallic particles and metals are directly precipitated from the solution which contains polyol. The adsorption parameters of the metal ions are strongly influenced by the factors such as temperature, quantity of adsorbent, pH and contact time. This method results in formation of metallic nanoparticles that are covered by a surface-adsorbed glycol which minimizes the oxidation. The magnetite nanoparticles of size ranging between 7-35 nm have been obtained using the polyol techniques by making the use of polyethylene glycol as solvent [133-135]. The third approach to produce nanoparticles involves decomposition of organo-metallic precursors done in the presence of hot organic solvents and surfactants known as thermal decomposition. This method shows good control over size, narrow particle size distribution, higher crystallinity and dispersibility. The morphology and size of synthesized particles can be controlled by reaction time, temperature and aging time. Since the particles are formed in the presence of large quantities of expensive and toxic surfactants, they need to be purified before biomedical applications. The particles with average particle size 4-60 nm are obtained using this method [136-138].

Another method known as hydrothermal or solvothermal method, involves wet-chemical techniques to crystallize the material in sealed container at higher temperature and vapor pressure. The particle sizes and their distribution are dependent upon the precursor concentration and hydrothermal treatment time. This technique yields very high quality end-products with narrow size distribution. Particles of average diameter 12-160 nm are reported by various groups with high temperature synthesis conditions [139-141]. The chemical vapor deposition method is used by researchers to synthesize one-dimensional or two-dimensional nanostructures such as nanotubes or thin films, respectively [142-143]. The precursors for reaction can be solid, liquid or in gaseous form at ambient conditions but they are supplied into reactor as a vapor.

The most commonly used nanoparticle synthesis technique is sol-gel method. This method involves hydrolysis and condensation process of metal alkoxides. The alkoxides are replaced with hydroxide group of water in hydrolysis step to generate a free alcohol. This technique involves the hydroxylation and condensation of the precursors present in the solution, which initiates the formation of a “sol” containing nanometric particles. Further condensation and additional inorganic polymerization leads to formation of metal oxide three dimensional network. The final crystallites are obtained after the heat treatment of the obtained gel. The factors such as precursors, temperatures, solvent type, pH, catalysts and the mechanical agitation play an important role in the growth kinetics, hydrolysis and condensation reactions. The magnetite nanoparticles with average size ranging between 8-17 nm have been obtained using this method which are further annealed at higher temperatures to obtain pure phase nanoparticles [144-146].

For our study, the liquid phase method involving microemulsion technique has been used to synthesize the magnetite nanoparticles. We have selected this method due to its ability to produce highly monodispersed, well crystalline nanoparticles. This method gives a superb control over the size and shape of nanoparticles. The mechanism, advantages and disadvantages of microemulsion technique has been discussed in detail in the following section.

2.4.1 Magnetite Synthesis via Microemulsion Technique

It is the isotropic dispersal of two thermodynamically stable and immiscible phases containing oil and water phase stabilized using a surfactant. The surfactant molecule is capable of forming a monolayer at the interface of water and oil, with hydrophilic groups towards the water phase and hydrophobic tails dissolved in the oil phase. The surfactant molecules possess amphiphilic nature which allows them to stabilize distinct microscopic systems of heterogeneous nature [147-150]. In the binary systems consisting of oil-surfactant and water-surfactant mixture, surfactants lead to formation of normal micelles with hydrophobic tails inside. In the case of reverse micelles, the hydrophilic parts points inside, along with certain aggregation numbers. For higher concentration of surfactant, different liquid crystalline phases are formed. The concentration and geometry of the surfactant molecules along with concentration of added salts and temperature decides the morphology of micellar aggregates. In case of ternary water-surfactant-oil system, a thermodynamically stable transparent solution, termed as ‘microemulsion’ is formed at certain conditions [150]. This microemulsion phase contains water and oil domains of nanosize range that are structurally well-defined and separated from each other by a single layer of surfactant film. The characteristic length and morphology depends on the ratio of water-to-oil and the elastic characteristics such as rigidity constants and spontaneous curvature of the surfactant layer. The microemulsions with droplet phase exist only if either water or oil phases exist in larger quantities but if both the phases are present in the solution in comparable amount, a bicontinuous microemulsion is formed [151].

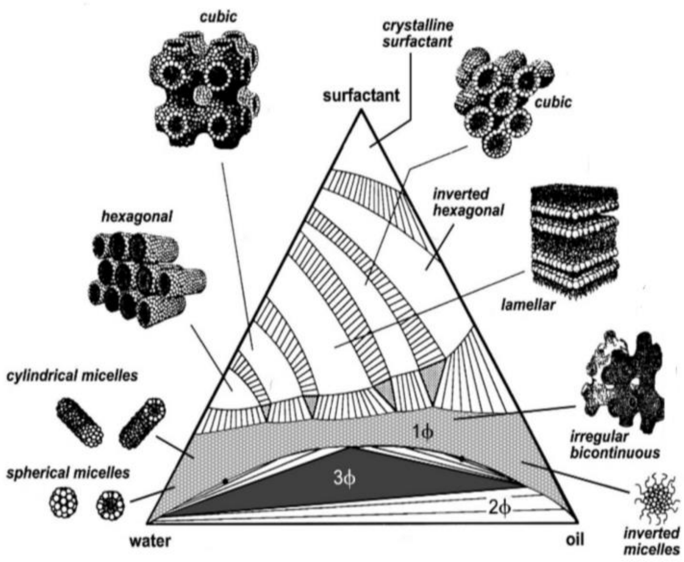

Figure 2.2 Schematic phase diagram that displays the existence regions of a variety of morphologically different self-assembled surfactant phases together with their multi-phase equilibria that can principally form in a ternary system of water, oil and a medium- or long-chain surfactant around its balanced state [151].

Figure 2.2 shows schematic ternary phase diagram that demonstrates various regions with distinct morphologies of different self-assembled phases of surfactant along with its multi-phase equilibrium formed in a water, oil and surfactant system. For smaller water to surfactant ratio, the micellar structure ranges from spherical to cylindrical form. The water-to-oil ratios for intermediate concentrations form an interwoven network oil and water channels whereas for higher concentration, the formation of cubic and hexagonal phases takes place, which consists of micelles and reverse micelles that aggregates leading to development of ordered crystalline arrays and crystalline lamellar liquid phases built by stack of bilayered surfactant sheets being separated by water or oil phases.

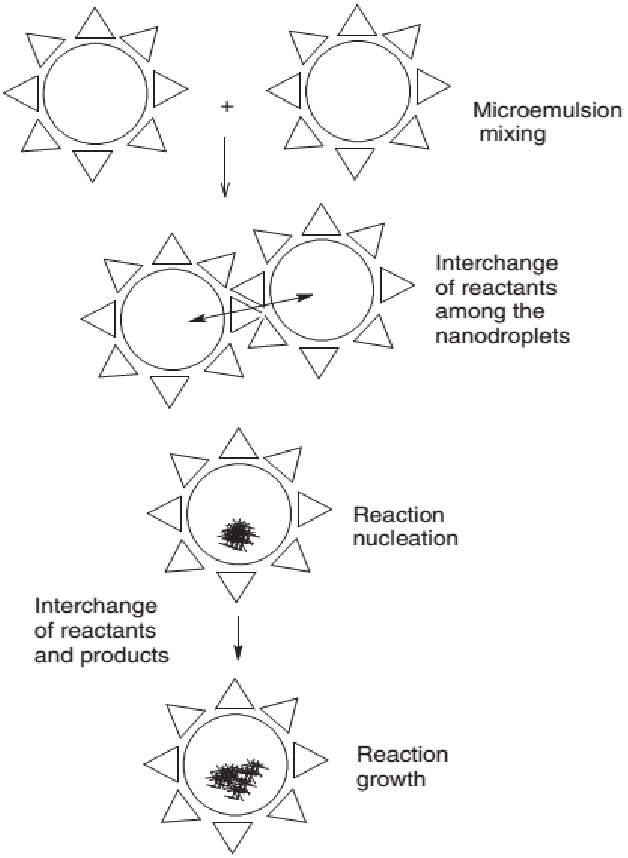

Figure 2.3 Different stages of the formation of nanoparticles [149].

The formation of nanoparticles in the microemulsions occurs in three different stages is shown in Figure 2.3 [149]:

- ***Chemical Reactions***: This is the instantaneous step that occurs within fraction of seconds after the addition of reactants inside the solvent. The domains inside the emulsion are constantly in motion and collide with each other. During every collision, an exchange of materials inside the domain takes place which leads to the chemical reactions leading to formation of a byproduct. The overall process of oil/ water domains motion and collision is characterized using a parameter τ_{ex}, that is characteristic for every microemulsion. The chemical reaction dynamics is a function of ratio between the characteristic time of chemical reaction (τ_r) to the exchange time (τ_{ex}). The distribution of dissolved salts inside the droplet follows Poisson distribution.

- ***Nucleation***:

The cage like effect provided by surfactant-stabilized cavities lead to controlled nucleation, growth and agglomeration. The occupation numbers of the reactants (solutes) in the aqueous droplet cores, the kinetics of the chemical reaction(s) leading to particle formation and the rate of solute exchange between the droplets governs the particle nucleation and growth [151]. On mixing the reactants, the micelles undergo Brownian motion causing energetic collisions that lead to mixing of micellar contents. When the number of molecules in single droplet exceeds the critical number of molecules ($N_{critical}$) required for formation of a stable nucleus, the new particles come into existence and process of nucleation starts.

- ***Particle Growth*****:** The smaller nuclei develop to large particle which is initiated via different mechanisms such as the dissolved reactant molecules are transported from one place to other by diffusion. The other mechanism involves convection to surface of particle which is followed by a reaction at the particle surface or aggregation of smaller nuclei. The first mechanism plays a major part in the growth of particles. This growth rate of particles is highly dependent on the concentration of dissolved salts.

The entire process of formation of nanoparticle via microemulsion is governed by certain rules [150-151]:

(i) The two non-empty and non-nucleated micelles/ droplets collide with each other that can lead to complete transfer of solute in single micelle and form an empty micelle.

(ii) The fusion occurs between two micelles with different reactants that results in complete mixing of solutes and reaction in one micelle and forms an empty micelle.

(iii) The collision between a non-nucleated and nucleated micelle causes complete transfer of solute in the micelle which contains nucleus and leads to growth of existing nucleus along with formation of another empty micelle.

(iv) The fusion of empty micelle with any micelle leads to no change.

The use of microemulsion technique to synthesize nanoparticles has many advantages along with few disadvantages:

Advantages

- An easy and precise control on particle size is achievable.
- The obtained nanoparticles have narrow particle size distribution.
- This method requires no high temperature treatment of samples, no pH control and is cost-effective.
- For synthesis of coated particles, it leads to development of uniform layer of shell material.

Disadvantages

- It comprises of a very complex system that includes huge amount of surfactant, co-surfactant in addition to oil phases.
- The separation of particles from emulsions and its purification are difficult processes.
- Very small quantities of particles are synthesized using microemulsion method.

The size and morphology of nanoparticles formed in microemulsions is guided by various parameters that includes water to surfactant molar ratio, the chemical nature of reagents, oil phase, mixing and polar volume fraction. To synthesize a nanoparticle of desired shape and size, certain practical conditions such as drying medium, type of surfactant, amount of surfactant, amount of iron salts used, molar ratio of metallic salts and synthesis temperature needs to be optimized.

In past years, many researchers have worked to optimize the synthesis conditions for microemulsion technique in order to obtain the pure phase nanoparticles. In 2007, W.F.C. Sager published a chapter as a part of lecture notes on microemulsion templating which dealt with the basic idea of defining ternary phase diagram to obtain the nanoparticles for different shapes and sizes [151]. The experimental conditions required for the formation of various self-assembled surfactant phases and correlation between the exchange kinetics with structural changes of droplet phases has been discussed. The synthesis of spherical and rod-like nanostructures from single and aggregated droplet phases is discussed in detail with several examples of inorganic materials. The chapter also focuses on the mechanisms involved in the formation of nanoparticles (nucleation and growth), main characteristics of microemulsions and effect of several parameters on particle shape and size. In the year 2004, Liu and Wang reported a method based on single microemulsion that acts as reaction mediator for the formation of magnetite nanoparticles with an average diameter of 10 nm [152]. The method was found to be very cost-effective and yields nanospheres with narrow particle size distribution as shown by transmission electron micrographs. The XRD and FTIR characterization were performed to confirm the structure and composition of obtained magnetite nanoparticles. H. Maleki, in 2012, reported the synthesis of gold coated superparamagnetic iron-oxide nanoparticles in the size range 7-10 nm using water in oil microemulsions with a narrower size distribution <2nm [153]. The effect of water-surfactant molar ratio, concentration of iron salts and reducing agent concentration on the crystallinity, size and shape of the nanoparticles has been studied. The size and shape of the nanomaterials are controlled by the micelles which need to be optimized. In 2015, Roman Latsuzbaia and co-workers proposed a design of synthesis strategy for the ultrafine metal nanoparticles by templating bicontinuous microemulsions [154]. The surfactant size has been reported to be the controlling factor for particle size. This strategy was demonstrated using various systems such as platinum and gold and also for different surfactants. The composition selection in the study was done after determination and rigorous study of the ternary phase diagram of the system. Several other findings on varying systems show more or less similar results [21,23,155-161]. This highlights the superiority of this method over other chemical methods for synthesis of monodispersed nanoparticle and its ease to obtain core-shell nanoparticles.

2.5 Characterization Techniques

2.5.1 Powder X-Ray Diffraction

The powder XRD method is an analytical technique used to study the structural properties of materials. It provides quick results and non-destructive analysis of the constituting elements without any kind of sample preparation. For the study of the synthesized samples in following chapters, a Miniflex (Rigaku, Japan) X-ray diffractometer using CuKα radiation has been used. The advantages of the X-ray powder diffraction method are (i) the diffraction pattern obtained from specimen is characteristic for given element or compound., (ii) the pattern produced by each substance in the mixture is their own and not dependent on others, and (iii) the qualitative and quantitative analysis of the distinct phases present in the mixture is possible through this method. This technique is used to identify and classify the presence of single or multiple phase structures in a material.

The XRD pattern, in addition to identify the crystal phases, can also be used to determine the crystallite size of the material. The peak broadening is influenced by crystalline domain size and strains. The calculation of this domain size, termed as crystallite size, is done using Scherrer equation [162]:$t = \frac{0.9\,\lambda}{\beta\, cos\theta}$. The further analysis of XRD using advance software such as FullProf is used to perform LeBail refinement of data which can further reveal the information about unit cell parameters [163]. XRD pattern for the samples under investigation is obtained in the 2 theta ranges of 20 to 80 degrees at room temperature in a step size of 0.02 degree.

2.5.2 Transmission Electron Microscopy

This is a microscopy technique in which a beam of electrons is transmitted through a very thin sample which interacts while passing through the sample. All the transmission electron micrographs reported in this work has been obtained from FEI TECNAI G2 20 TWIN Type Transmission Electron Microscope, FEI, USA, operating at 200 kV.

The TEM has been developed to overcome the limitation of maximum resolution provided by a light microscope. These incident electrons interact with each material in a different way due to variation in electron densities which may produce a contrast in a high resolution image of single nanoparticle that is helpful in determination of core-shell structures. The samples used for TEM imaging should be ultrathin and must withstand impact of high energy electrons as well as high vacuum. The powder samples under observation are first dispersed in a suitable solvent such as ethanol by sonication for few minutes. A drop of the solution is then casted on a commercially available copper grid with help of a fine tip syringe or micropipette. The grid is then dried in vacuum at 40 ^{0}C for few hours. This grid is used in transmission electron microscope for imaging purposes.

The TEM is also equipped with EDXS (Energy Dispersive X-ray Spectroscopy) which helps in elemental analysis and chemical characterization of the material. On focusing the sample with high voltage electron, an electron in its ground state gets excited in a distinct electron shell which creates an electron hole. The electrons from higher energy levels come to lower state in order to occupy the generated electron hole. The energy difference between two levels is released in form of X-ray which is a characteristic for every element.

2.5.3 SQUID Magnetometry

A Superconducting Quantum Interference Device (SQUID) magnetometer is employed to measure the magnetic properties of the materials in a wide range of temperature and applied magnetic field. It is considered as an ideal instrument to investigate about the magnetic properties of nanoparticle system due to its extremely high sensitivity. The measurements such as time and field dependent magnetization, ac susceptibility, magnetic spin relaxation and magneto-caloric effect can be performed using the instrument. SQUID Magnetometry requires superconducting coil to operate which is done by use of liquid helium and liquid nitrogen that is also helpful in conducting experiments in low temperature environment for superparamagnetic materials. The magnetometer measures the changes experienced in magnetic flux, which is then converted and measured in form of current, due to movement of sample through superconducting detection coil. The magnetic measurements in this study have been performed using a Magnetic Properties Measurement System (Quantum Design®, USA). The DC magnetization measurements of the samples were carried out using this setup in the magnetic field range of ±7 Tesla. The experiments were done using standard protocols for zero-field-cooled (ZFC) and field-cooled (FC) measurements. The temperature raise for the experiment from 2 K to 300 K was done in a step size of 0.02 K. The hysteresis loops of the sample were recorded at temperatures 5 K and 300 K in magnetic field range of ±7 Tesla. The magnetic properties of materials can be measured in powder or pellet form. The ac magnetic susceptibility of the synthesized magnetite nanoparticles has been measured for frequency ranging between 10 Hz to 1000 Hz. The magnetic spin relaxation for the synthesized nanoparticles has been measured at temperature 2 K under an applied magnetic field of intensity 50, 100, 500, 1000 and 2000 Oe.

2.5.4 UV-Visible Spectroscopy

The UV-Visible spectrometer is used to obtain the absorption spectrum for liquid or solid samples when illuminated by the light in ultraviolet-visible region. The absorbed or reflected wavelength in visible spectral region corresponds to the colour shown by the material. It is the region in electromagnetic spectrum, where molecules or atoms undergo the corresponding electron transitions. The dual beam UV–Visible (UV-Vis) spectrophotometer (Hitachi, U-3010) has been used to study the absorption properties of the material synthesized in this study.

The spectrometer measures the ratio of intensity of light after passing the sample to light intensity before passing the sample. This ratio of intensity is termed as transmittance. The transmittance value obtained using the spectrometer is converted to absorbance using Kubelka-Munk equation. The dual beam spectrophotometer splits the light into two beams before it reaches the sample. One of the beam passes through the sample and the other one is used as reference. The intensity of beam that passes through reference is considered to be 100% transmission or zero absorbance. The measured value is the ratio of intensities of the two beams. The UV-Vis spectroscopy is also helpful in determining the path length and concentration of the material dissolved in the solvent by the use of Beer-Lambert law. The energy band gap of the samples can also be estimated by the use of tauc equation.

2.5.5 Photoluminescence Spectroscopy

It is a spectrometer which uses non-destructive and non-contact means to probe about the electronic structure of the materials. It involves a process in which light of certain wavelength is illuminated on the sample which gets absorbed and photo-excitation of material takes place. In this process, the valence band electrons absorb the energy and jump to higher electronic states, release the energy in form of photons to relax and then return back to the lower energy level. The light emitted during this process is termed as photoluminescence (PL) and the instrument used to study the PL phenomena is termed as photoluminescence spectrometer. The luminescence spectra for the samples involved in this study has been recorded by use of two different PL spectrophotometer: Hitachi F-4600 Fluorescence spectrometer (Xenon lamp as excitation source) and FLSP-900, Edinburgh Instruments, UK) equipped with 450 W Xenon lamp as excitation source. The quantum efficiencies of the samples have also been calculated by use of an integrating sphere equipped with spectrometer FLS900 (Edinburgh Instruments, UK).

The PL spectrometer can be used in wide range of applications from recording emission and excitation spectra for a particular wavelength to determination of band gap, detection of impurity and defect levels as well as to study the recombination mechanism of electron-hole in the material. The excitation spectra of the samples are recorded by monitoring the emission at constant wavelength and while varying the wavelength of excitation. For emission spectra, a light of fixed wavelength is irradiated on the sample to excite it. The intensity of the emitted radiation is recorded as the function of wavelength which represents emission spectra.

2.5.6 Particle Size Analysis

This is a type of characterization technique which is used to determine the size distribution of particles in a given liquid sample. For the solid samples, the material has to be suspended or dispersed in an appropriate solvent. It uses dynamic light scattering to analyze the particle size by measuring the Brownian motion of suspended particles or molecules in the solution. For larger particle sizes, the Brownian motion will be slower. This method monitors the Brownian motion of the particles with light scattering. The fluctuations in the scattered light intensity are measured for a given period of time where the processed data is given as auto-correlation function. Another analysis performed on auto-correlation function termed as ‘polydispersity analysis’ gives the size of particles along with the number of particles with each size. The dynamic range for the instrument is generally 0.3 nm-8 μm. The size and size distribution of samples in the current study were done by Dynamic Light Scattering (DLS) method using Horiba Scientific nanopartica SZ-100 series (Horiba, Japan).

The particle size analyzer is also helpful in characterization of surface charge of the particles by measuring their zeta potential. The sample in form of liquid is inserted inside a disposable electrode cell and the particle electrophoretic mobility is measured which gives calculated zeta potential. The larger magnitude of zeta potential indicates the higher stability of nanoparticles.

2.5.7 Hyperthermia Measurement

The hyperthermia measurement is performed on a setup that consists of a radiofrequency coil to generate electromagnetic field and a thermometer. The study has been performed at a frequency 737.9 kHz & 110 kHz and magnetic field amplitude 17 mT & 25 mT, respectively, for different samples under observation dispersed in oleic acid with variable concentrations.

The samples with single domain, on application of an alternating magnetic field, generate heat via Neel and Brownian mechanism which is helpful in hyperthermic treatment of abnormal tissues and cells. The elevated temperatures for given concentration of samples and alternating magnetic field are recorded using the temperature probe.

2.5.8 ICP-MS

Inductively coupled plasma mass spectrometry (**ICP-MS**) system is a type of mass spectrometer which uses an inductively coupled plasma to ionize the sample under observation. It is used to detect metals and several non-metals in liquid samples at very low concentrations. The elemental analysis of the silver coated magnetite nanoparticle samples were performed on ICP-MS system, Agilent 7900.

2.6 Synthesis Protocols for Magnetite Nanoparticles

The used chemicals ferrous ammonium sulphate, Triton-X and sodium hydroxide were obtained from Himedia having minimum assay of 99%, 99% and 98%, respectively. The ferrous ammonium sulphate from MP chemicals with purity 98%, sulphuric acid (Rankem, assay 97%) and CTAB from Loba Chemie with minimum assay 99% were used in synthesis procedures. The 18.2 MΩ Milli-Q water obtained from Merck was used in entire synthesis and washing processes. The chemicals were used as received from the supplier without any further purification.

A solution of iron oxide salts- ferrous and ferric ammonium sulphate is freshly prepared by addition of calculated amounts with various molar concentration and molar ratio 1:2 in 10 ml of 0.4 M aqueous H_2SO_4 (Solution 1). A second solution with NaOH (1M/ 2M) and surfactant Triton-X and CTAB with pre-determined molar concentrations is prepared in 40 ml of distilled water (Solution 2). This solution is stirred and heated for half an hour in a constant temperature water bath at reaction temperature (50-80 ^{0}C for different sets). The solution 1 containing iron salts is added in solution 2 drop by drop along with constant heating and stirring. The solution is kept in the same condition for additional one hour after mixing of solution 1. The Fe_3O_4 nanoparticles obtained as black precipitate settles at the bottom of vials within few minutes. The solution is

TABLE 2.1. Summary of synthesis parameters for magnetite nanoparticles using micro-emulsion. The variable parameter is indicated in bold letters.

S. No.	**Varying Parameters**		**Fe^{+2} Conc. (M)**	**Fe^{+3} Conc. (M)**	**Surfactant Conc. (M)**	**Reaction Temp (^{0}C)**	**Iron Stock Solution Used (ml)**
1	Drying medium	**air**	0.09	0.18	0.1	72	4
		vacuum	0.09	0.18	0.1	72	4
2	Type of Surfactant	**TX-100**	0.05	0.1	0.1	72	8
		CTAB	0.05	0.1	0.1	72	8
3	Molar Ratio of Surfactant		0.05	0.1	**0.01**	72	8
			0.05	0.1	**0.05**	72	8
			0.05	0.1	**0.1**	72	8
4	Concentration of Iron Salts		**0.05**	**0.1**	0.1	72	4
			0.09	**0.18**	0.1	72	4
			0.25	**0.5**	0.05	72	4
5	Synthesis Temperature		0.09	0.18	0.05	**55**	5
			0.09	0.18	0.05	**60**	5
			0.09	0.18	0.05	**65**	5
			0.09	0.18	0.05	**72**	5
			0.09	0.18	0.05	**80**	5

further washed several times with ultrapure water using sonication and centrifugation. The synthesized nanoparticles are then dried in air or vacuum (for different sets) at reaction temperature ranging between 55-80 ^{0}C for another 24 hours. The synthesis processes involved for obtaining magnetite nanoparticles is shown as flow chart in Figure 2.4. The reaction parameters for synthesis of magnetite nanoparticles were varied for various sets in order to optimize the conditions according to the **Table 2.1**.

The synthesis in emulsion gives Fe_3O_4 nanoparticles with narrow size distribution which can easily be segregated from byproducts obtained during the reaction by centrifuging the solution. The particle size obtained with this method is comparatively smaller than those obtained by other chemical route methods and has good reproducibility.

We will now discuss the role of each synthesis parameters.

2.7 Effects of Synthesis Parameters on Size and Shape of Nanoparticles

The synthesis parameters such as drying medium, type of surfactant, molar concentration of surfactant, concentration of iron salts and reaction temperature play a crucial role in deciding the crystallinity, phase purity, shape and size of the synthesized nanoparticles. The role of each parameter has been discussed in details.

2.7.1 Effect of Drying Medium

The drying medium plays an important role in the phase purity of the prepared samples. It becomes crucial when the prepared samples are susceptible to oxidation and phase decomposition. A set of two samples were prepared under same synthesis parameters and reaction conditions except the drying medium. One of the two samples was dried in presence of air whereas the second sample has been dried in vacuum at same temperature.

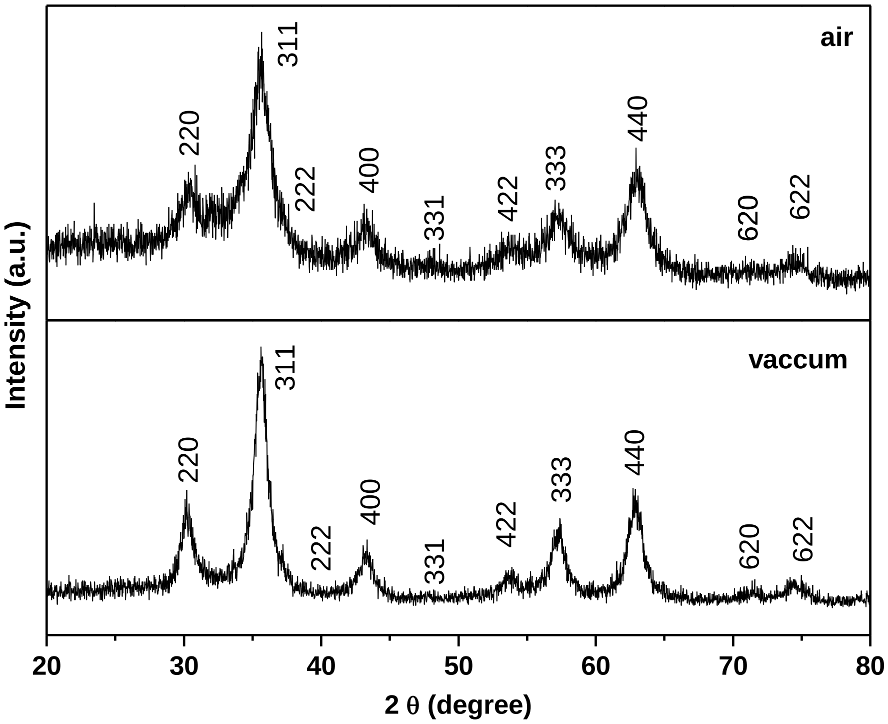

Figure 2.4. XRD Patterns of Fe_3O_4 dried in presence of air and vacuum.

Figure 2.5 shows the role of drying medium on the phase purity of the Fe_3O_4 nanoparticles. It can be seen that; though same synthesis conditions have been used, samples dried under vacuum were much crystalline in nature and in pure phase when compared to those dried in presence of air (Fig.2.5) indicating that an inert or vacuum environment is preferable.

2.7.2 Role of Surfactant

The nanoparticles formation and their dispersion are highly influenced by type of surfactant used in synthesis. Taking reference of surfactants used in earlier experiments performed by several researchers, Triton X has been used as surfactant for comparative study with CTAB.

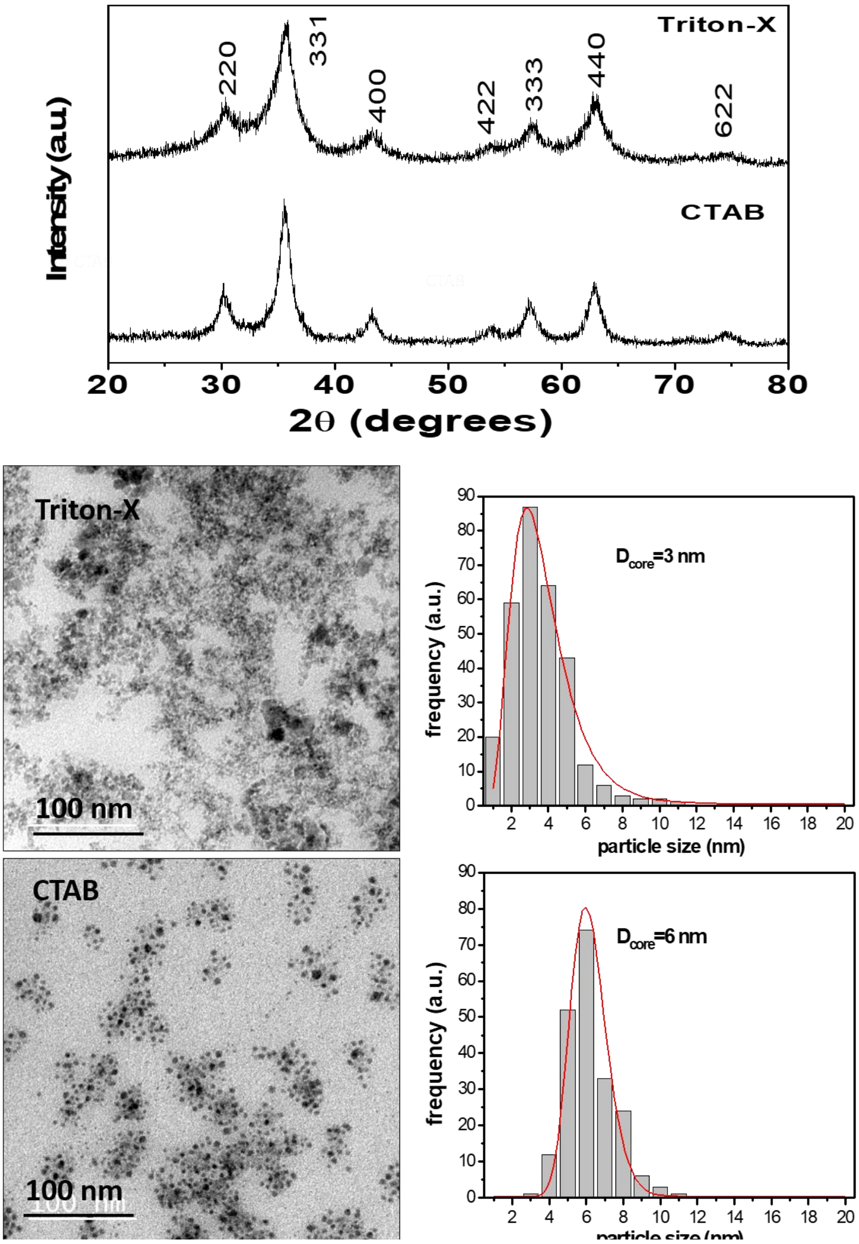

Figure 2.5. XRD and TEM images of magnetite nanoparticles synthesized using surfactants Triton X- 100 and CTAB.

Figure 2.6 shows the X-ray diffraction pattern (XRD) and TEM images for nanoparticles synthesized in presence of two different surfactants Triton-X and CTAB while keeping all the other synthesis parameters same. The particles obtained in presence of TX-100 were smaller in size (~3 nm) and showed diffused rings in the

SAED indicating their amorphous nature. The magnetite nanoparticles obtained using CTAB as surfactant was found to be comparatively larger in size (particle size ~7 nm) for same molar concentration of CTAB as that of Triton-X but are found to show better crystallinity. The nanoparticles formed in Triton-X are heavily agglomerated. This shows that the CTAB as a surfactant is performs better in comparison to Triton-X. Thus, use of CTAB as surfactant has been preferred for further synthesis procedures.

2.7.3 Role of Surfactant Molarity

Another set of samples keeping all the reaction conditions and synthesis parameters constant except the surfactant molarity was obtained. On further analysis of the nanoparticles using XRD graphs and TEM images, it was observed that nanoparticles synthesized under different molar concentrations of surfactant CTAB leads to change in the shape of particles without having much effect on their particle size. The shape of the nanoparticles is found to be cubic (fig 2.7 (a)), nearly pentagon (fig 2.7 (b)) and spherical (fig 2.7 (c)) for molar concentration of CTAB as 0.01 M, 0.05 M and 0.1 M, respectively. This change in shape of nanoparticles can be attributed to the difference in nanodroplets morphology having its origin in water- to -surfactant ratio which is observable from the ternary phase diagram for oil-water-surfactant microemulsion. This study revealed the area of phase diagram on scale of surfactant which should be focused for synthesis of nanoparticles with desired shape and size.

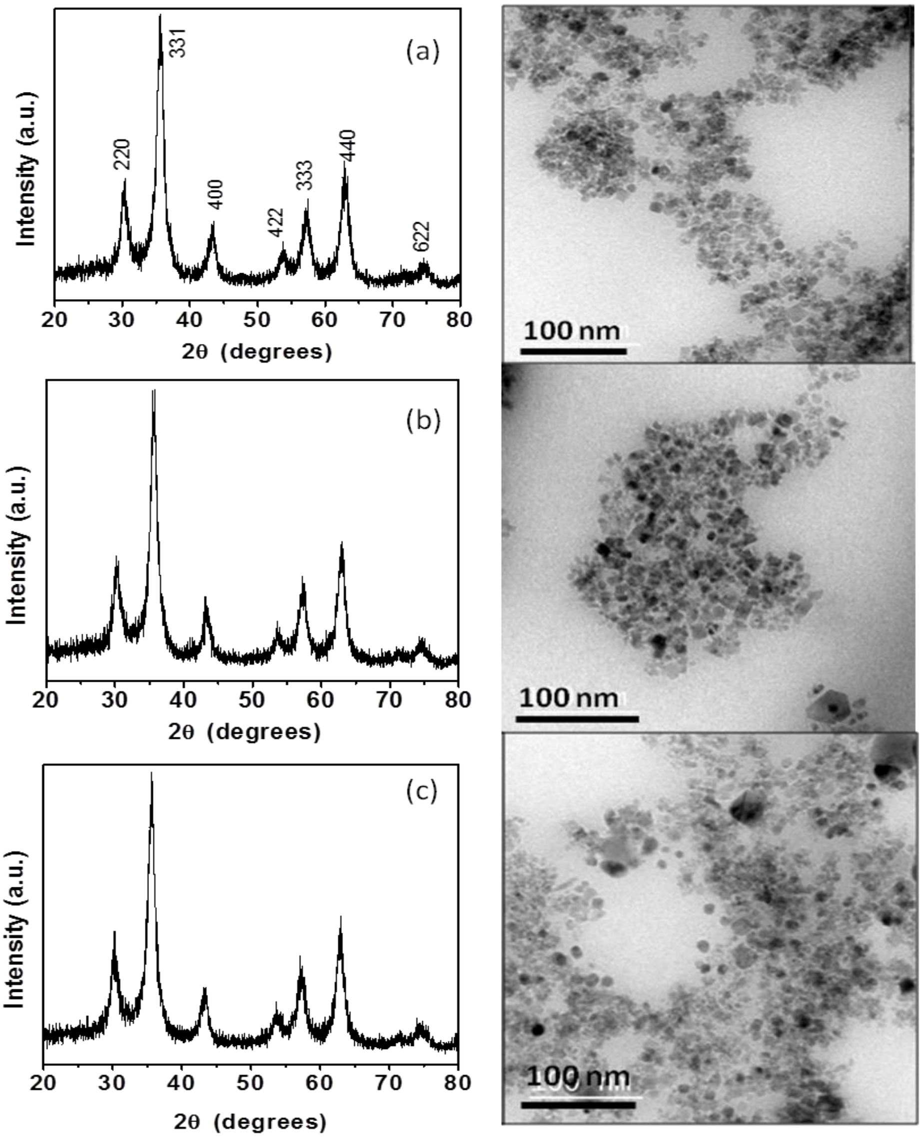

Figure 2.6. XRD and TEM images of Fe_3O_4 nanoparticles under different molar concentration of surfactant CTAB (a). 0.01 M, (b) 0.05 M and (c) 0.1 M; representing change in particle shape of the nanoparticles with increasing concentration.

2.7.4 Concentration of Iron Salt

A set of three samples were produced for different molar concentrations of iron salts to study its impact on the formation of magnetite nanoparticles. The development of single

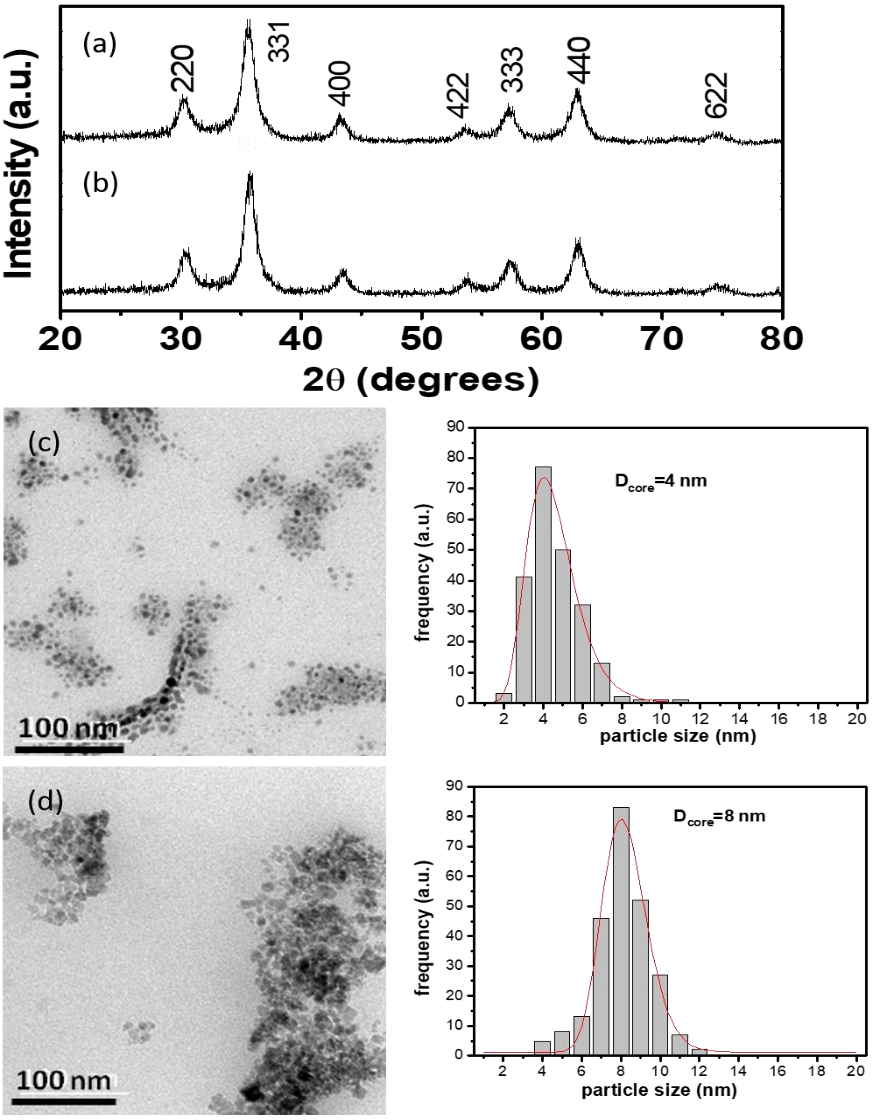

Figure 2.7. XRD and TEM images of Fe_3O_4 nanoparticles under different molar concentrations of ferrous-ferric salts (a) & (c) Fe^{2+}=0.05 M, Fe^{3+}=0.1 M; (b) & (d) Fe^{2+}=0.09 M, Fe^{3+}=0.18 M.

phase Fe_3O_4 nanoparticles depends on the molarity of ferrous-ferric salts present in the solution. The particles are formed in single phase for lower molar concentrations of iron salts whereas some extra phases of α-Fe_2O_3 were observed for relatively higher molar concentration. The concentration of iron salts also has a crucial effect on the size of the particles. The nanoparticle size increases from ~4 nm to ~8 nm (fig 2.8 (a)& 2.8 (b)) when the concentration of ferrous and ferric salts are varied from 0.05 M to 0.09 M for ferrous salts and 0.1 M to 0.18 M for ferric salts, respectively, keeping all the other parameters of synthesis fixed for the sample set. For 0.25 M Ferrous salt concentration and 0.5 ferric salts molarity, extra phases of α-Fe_2O_3 were identified from XRD data.

2.7.5 Synthesis Temperature

A set of five samples were synthesized to decide the optimum temperature range for obtaining pure phase magnetite nanoparticles. The synthesis method for Fe_3O_4 nanoparticles were repeated for various reaction temperatures, i.e., 55°, 60°, 65°, 72°

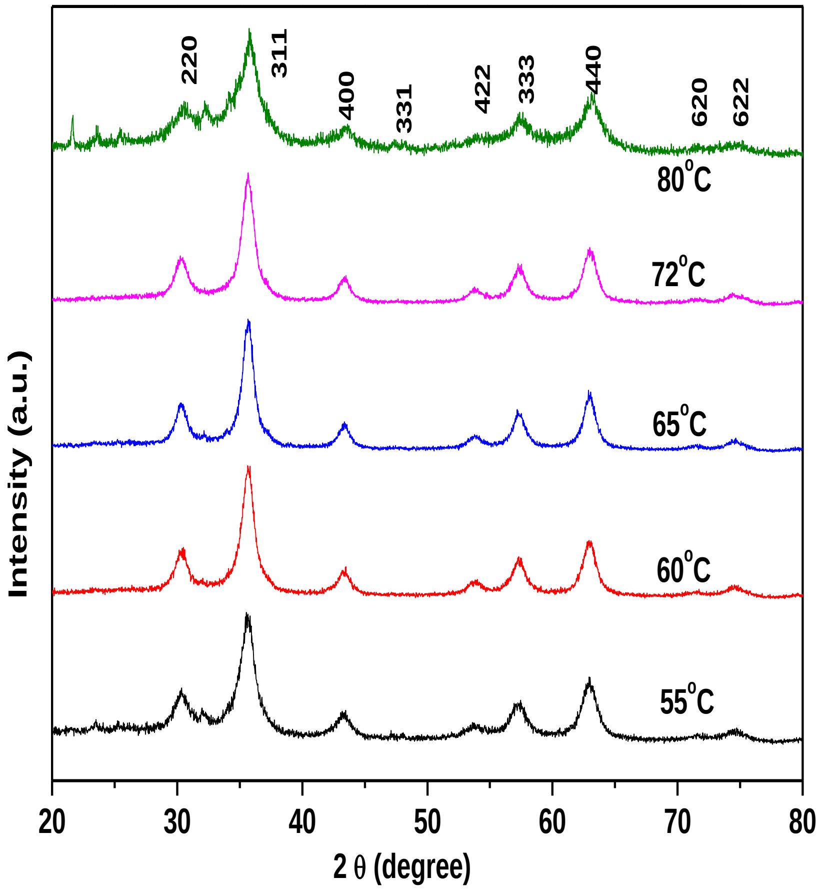

Figure 2.8. XRD pattern of Fe_3O_4 nanoparticles synthesized at different reaction temperatures.

and 80^0C. The XRD pattern of the samples in fig 2.9 indicate that the particles can be synthesized with better crystalline nature and single phase between the reaction temperature 65^0C-72^0C. The crystallite size was found to be 7 nm to 8 nm for samples synthesized in the reaction temperature range of 65^0C-72^0C.

A unified methodology (microemulsion technique) to produce pure Fe_3O_4 nanoparticles of distinct shape and sizes by varying physical and chemical parameters such as reaction temperature, molar concentration, etc has been identified. The advantage of this process is lower synthesis temperature, no inert atmosphere and no pH regulation. The obtained particles show narrow size distribution and good reproducibility. As a result, CTAB is a commendable surfactant as compared to Triton-X giving less aggregated particles. The synthesis temperature to obtain best results is found to be 65-72°C.

2.8 Synthesis of Magnetite- Silver Core- Shell Nanostructures

Silver coated magnetite nanoparticles were obtained as a separate process after the formation of magnetite nanoparticles as shown in Figure 2.10. The magnetite nanoparticles are weighed and calculation in order to derive the quantity of silver nitrate required for complete coating of the magnetite nanoparticles with pre-determined shell thickness. The magnetite nanoparticles are dispersed in 100 ml of ultrapure water for about 2 hours through ultrasonication. The dispersed solution is kept in a constant temperature water bath of 50^0 C with constant magnetic stirring. 100 mg of glucose, 1 M of NaOH and CTAB are added to the solution and allowed to mix for 15 minutes (solution 3). The amount of CTAB used is in molar ratio 1:1 with silver nitrate. Calculated amount of $AgNO_3$ dissolved in 10 ml of water is mixed in the solution 3 drop-wise and kept at constant stirring with same temperature for another 24 hours. The change in colour of black mass to grey indicates the formation of coated magnetite nanoparticles. The suspension obtained are further washed and separated from the

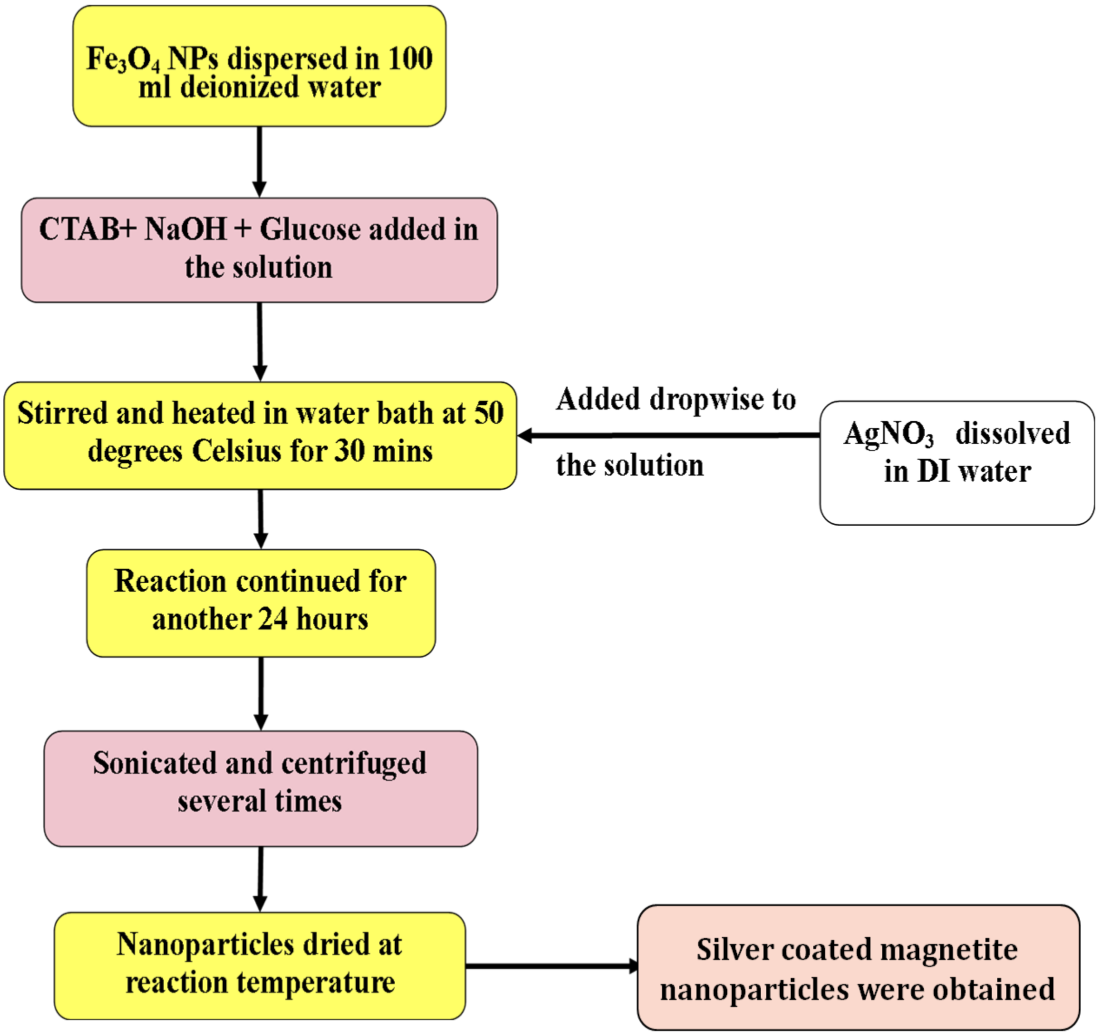

Figure 2.9 Process for obtaining silver coated magnetite nanoparticles.

solution and followed by drying at 50^0 C for next 24 hours in vacuum. The use of CTAB is done to ensure uniform silver coating on magnetite nanoparticles while glucose is employed to eliminate the formation of silver nanoparticles individually.

The silver nitrate was procured from Central Drug House Pvt. Ltd. with assay 99.8% whereas glucose was obtained from Himedia having purity of 99.5%. All the other chemicals used in coating of magnetite nanoparticle are same as described earlier. The chemicals were used as received without any further purification. The shell thickness of silver covering the magnetite nanoparticles has been controlled by varying the quantity of silver nitrate in the solution.

2.9 Synthesis of Janus Shaped Silver-Magnetite Nanoparticles

The synthesis of Janus shaped silver-magnetite nanoparticles is carried out in two steps as reported in earlier section for core-shell structure with minor modifications. The magnetite nanoparticles are weighed and dispersed in distilled water. The amount of silver nitrate required to coat the magnetite with desirable shell thickness was calculated, weighed and mixed in distilled water. NaOH and glucose were added to the magnetite solution. In this solution, the silver nitrate solution is mixed drop by drop. The mixed solution is allowed to heat at temperature 50 ^{0}C and stirred for another 12 hours. The silver-magnetite nanoparticles are washed and separated from the solution. The nanoparticles obtained are dried at reaction temperature i.e. 50 ^{0}C in vacuum.

2.10 Conclusion

To conclude, the physical and chemical parameters of nanoparticles are crucially affected by the synthesis parameters. A systematic study on role of different associated parameters of microemulsion synthesis method on the formation of Fe_3O_4 nanoparticles is performed. From X-ray Diffraction and Transmission Electron Microscopy data analysis, the size of synthesized particles was observed to be <10 nm. The critical concentration of ferrous- ferric solution to obtain particles in single phase has been found to be ≤ 0.09 M and ≤ 0.184 M, respectively. The variation of molar concentration (0.01 M $\leq x \leq$ 0.1 M) of CTAB leads to formation of Fe_3O_4 nano-scale particles of distinct morphologies e.g. nano-cubes, pentagons and spheres. The number of ferrous and ferric ions involved in the formation decides the size of the nanoparticles. The single crystallographic phase is obtained in reaction temperature range of 65^0 C<T< 72^0

C. The method facilitates to produce nanostructures having narrower size distribution along with good reproducibility.

Since the nanoparticles for biological applications has to be in the range of particle size below 40 nm, and it should also exhibit desired properties for multimodal imaging. The very first criterion for multimodal application is having surface plasmon resonance in the visible range of the optical spectrum. It is therefore desirable to first determine the size range for core-shell nanoparticle system, through theoretical means, for magnetite core and Ag/Au shell. In the next chapter, a theoretical investigation for magnetite nanoparticles with core size ranging from 1 nm to 50 nm and gold/ silver shell thickness 1 and 2 nm has been carried out to estimate their SPR wavelengths. This helps in determination of the critical size range of core and shell thickness to obtain SPR properties and further tune them in entire visible range.